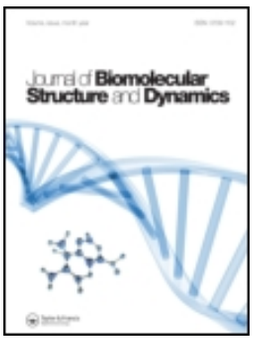

Journal of Biomolecular Structure and Dynamics

ISSN: 0739-1102 (Print) 1538-0254 (Online) Journal homepage: http://www.tandfonline.com/loi/tbsd20

Structural and Dynamic properties of a new Amyloidogenic chicken cystatin Mutant I108T

Yuanyuan Yu , Yaofeng Wang , Jianwei He , Yuan Liu , Hui Li , Huili Zhang & Youtao Song

To cite this article: Yuanyuan Yu , Yaofeng Wang , Jianwei He , Yuan Liu , Hui Li , Huili Zhang & Youtao Song (2010) Structural and Dynamic properties of a new Amyloidogenic chicken cystatin Mutant I108T, Journal of Biomolecular Structure and Dynamics, 27:5, 641-649, DOI: 10.1080/07391102.2010.10508578

To link to this article: http://dx.doi.org/10.1080/07391102.2010.10508578

Published online: 21 May 2012.

Journal of Biomolecular Structure & Dynamics, ISSN 0739-1102
Volume 27, Issue Number 5, (2010)

Structural and Dynamic Properties of a new Amyloidogenic Chicken Cystatin Mutant I108T

http://www.jbsdonline.com

Yuanyuan Yu[1]
Yaofeng Wang[2]
Jianwei He[1,2]
Yuan Liu[1]
Hui Li[1,2]
Huili Zhang[2]
Youtao Song[1,2,*]

[1]College of Life Science, Liaoning University, Shenyang 110036, China
[2]Province Key Laboratory of Animal Resource and Epidemic Disease Prevention, Shenyang 110036, China

Abstract

Chicken cystatin variant I108T is a mutant in the hydrophobic core of the molecule. It has shown many amyloid-prone characteristics in our previous experimental study. To explore the detailed structural and dynamic properties of the amyloidogenic mutant I108T, 10 ns molecular dynamic simulations of the I108T mutant and wild-type chicken cystatins were performed in this study. Our results suggested that the I108T mutant, which exhibited larger secondary structural fluctuations and hydrophobic core expanding tendency compared with the wild-type chicken cystatin, is a new amyloidogenic form of chicken cystatin, and therefore supported the hypothesis to some extent that site mutations in the hydrophobic core might induce the domain swapping.

Key words: Chicken cystatin; Molecular dynamic simulation; Amyloidosis; Hydrophobic core; Domain swapping.

Introduction

The cystatins are tight and reversible binding inhibitors of the papain-like cysteine proteinases. They form a superfamily of sequentially homologous proteins, of which human cystatin C (HCC) and chicken cystatin (cC) are representative (1, 2). A leucine 68 to glutamine variant (L68Q) of human cystatin C (HCC) is believed to be the causative agent of an amyloidotic disease, hereditary cystatin c amyloid angiopathy (HCCAA), which is a dominantly inherited disorder characterized by tissue deposition of amyloid fibrils in blood vessels (3). The L68Q variant can form highly domain-swapped dimers at physiological protein concentrations, thus forming part of the amyloidgenic deposits in the brain arteries, which may lead to fatal cerebral hemorrhage and cause death in young adults (4, 5).

Unfortunately, HCC monomers are extremely unstable in pathological conditions and there are only dimers present, which prevented us to study the mechanism of domain swapping (6, 7). Chicken cystatin (cC) has a number of similar structural characteristics to HCC. More importantly, cC has the experimental convenience over HCC of a higher thermodynamic stability for the folded state (8), and cC monomers are present in physiological condition. This advantage makes cC protein ideally suited for further studying the mechanism of cystatin c-type amyloidogenesis at the molecular level (9). Recently, cC model has been used by more and more researchers to study the mechanism of domain swapping and amyloid formation (9–11).

Abbreviations: MD: HCC - Human cystatin C; cC - Chicken cystatin; WT - Wild-type; I108T - An isoleucine 108 to threonine mutant of cC; I66Q - An isoleucine 66 to glutamine mutant of cC; L68Q - A leucine 68 to glutamine mutant of HCC.

*Phone: +86-24-62202280
Fax: +86-24-86864476
E-mail: ysong@lnu.edu.cn

Structurally, similar to HCC, each cC consists of a large five-stranded anti-parallel β-sheet wrapping around a central β-helix. The connectivity within the β-sheet is: (N)-β1-(α)-β2-L1-β3-(AS)-β4-L2-β5-(C), where AS is a broad 'appending structure' unrelated to the compact core of the molecule (12). Residue 66 in cC, corresponding to residue 68 in HCC, is located in the hydrophobic core of the protein molecule. Research on cC variant I66Q has confirmed that I66Q has similar amyloidogenic capacity compared with HCC L68Q under physiological conditions (9). By using the cC model that is thermodynamically stable, Sanders *et al.,* have revealed that under conditions leading to the formation of amyloid deposits, cystatin forms a tetramer through structural rearrangement of domain-swapped dimers prior to amyloidogenesis (8).

Interestingly, our previous study also revealed that the nonglycosylated form of I108T, another mutant in the hydrophobic core in cC, showed a blue shift in the far-UV circular dichroism (CD) spectroscopy analysis compared with that of the wild-type (WT) cC. The result indicated that the helix content decreased obviously in protein structure in the I108T mutant (11). In addition, similar to I66Q, the thioflavin T (a fluorophore widely used to detect amyloid structure in proteins) fluorescence value of I108T showed remarkable increase after 18 days of incubation. Furthermore, typical amyloid fibrils were clearly observed for the nonglycosylated form of I108T in the electron microscopy (EM) after 35 days of incubation, while no fibrils were observed for the WT cC (11). Such effects were found to be similar in amyloid mutant protein I66Q (11). These surveys suggested I108T might be a new amyloidogenic cC mutant. Nevertheless, up to now, detailed structural and dynamic information, which would be useful to illustrate the mechanism of amyloid aggregation, has yet not been investigated.

Molecular dynamics (MD) simulations can provide more detailed information on structural change at atomistic level and has been widely used in the amyloid protein studies. Several MD studies on amyloid peptides and proteins reported recently in this Journal (33, 35-39) explore their structural stability and aggregation behavior. Previous studies using MD simulations on HCC have revealed that the atomic details about the conformational change of HCC are responsible for the early stages of amyloid formation (13). Recently, Liu *et al.,* have studied the domain swapping mechanism of HCC through MD simulations (14). They reported that the interior hydrophobic core of the L68Q variant is relatively unstable, resulting in domain swapping more readily compared to WT HCC under conditions favoring this process.

Yet up to now, the monomeric model used in HCC study is homologously constructed based on the known X-ray crystal structure of dimeric HCC (PDB entry 1G96), while there is no way to verify its accuracy. Fortunately, the monomeric structure of cC has been confirmed by X-ray crystallography and nuclear magnetic resonance (NMR) spectroscopy (12), which enables us to apply MD simulation studies in I66Q variant, and the results matched well the experimental data in our previous study (15, 16).

Therefore, in order to further investigate the structure and dynamic characteristics in I108T mutant, we have performed several 10-ns-long molecular dynamics simulations of the cC I108T mutant in this study taking the WT cC as the comparison. Our computational methods complemented the experimental approaches to study the conformational changes of the new mutant I108T at the atomic level during the early stage of cystatin amyloid fibrils formation. These results may help us reveal the inherent properties of the new amyloidogenic-prone chicken cystatin mutant I108T and obtain new insight into the effect of site mutation of the hydrophobic core on amyloidosis mechanism.

Materials and Methods

Construction of I108T Mutant cC Monomer Models

The model of the monomeric molecule used in our work is based on the X-ray crystal structure of the coordinate of monomeric chicken cystatin (PDB entry 1CEW), which was obtained from RCSB protein data bank (2). The model of I108T monomer was constructed using homologous modeling method through the online service of Swiss Model (http://swissmodel.expasy.org/) (17-19).

Molecular Dynamics Simulations

All molecular dynamic (MD) simulations were performed using Gromacs 4.0 program (20-23) at the Supercomputer Center of Liaoning University (SCLU) on dual-core Pentium 2.8G processor of Linux cluster. GROMOS96 43a1 (24) force-field parameters were used in all simulations in this study. The time-steps were 2 fs throughout the whole simulations. The bonded interactions were calculated at every time-step, the short-range nonbonded interactions at every two time-steps, and the long-range electrostatics interactions at every four time-steps. The pair-list of the nonbonded interaction was recalculated every 20 time-steps with a pair-list distance of 14 Å. The short-range nonbonded interactions were defined as van der Waals and electrostatics interactions between particles within 12 Å. A smoothing function was employed for the van der Waals interactions at a distance of 10 Å. The particle mesh Ewald (PME) method (25, 26) was used for full evaluation of electrostatic interactions. Periodic boundary conditions and water wrapping were activated in the simulations. The SHAKE routine with a tolerance of 10^{-5} Å was used in all simulations.

Each monomer model was solvated in a water box containing 10124 spc216 water molecules (27) and neutralized by adding 14 Cl^- counterions. The minimum distance of a protein atom to the edge of the water box was 10 Å. The solvated and neutralized systems were then energy-minimized for 20 ps. Afterwards, the backbone atoms of the structure were fixed, while the side chains and solvent were allowed to move unrestrainedly for further 10 ps, followed by totally unrestrained equilibration for 12 ps, at constant temperature 300k (Langevin damping dynamics) and 1 atm pressure (Langevin piston pressure control) within a water box using periodic boundary conditions in the NPT ensemble. After equilibration the productive run was carried out at 330 K, pH2 for 10 ns. The atomic coordinates and velocities were saved every 1 ps, and coordinate trajectories were saved every 0.5 ps for subsequent data analysis.

Analysis of the Trajectories

The secondary structure of the protein was determined by DSSP program (28). Visual Molecular Dynamics (VMD) and pymol program (29) with home-developed scripts were used for system visualizations and other analyses. The root mean square deviations (RMSD) were calculated for all alpha-carbon (C) atoms with reference to the first frame of the trajectories.

Results and Discussion

Dynamics of I108T Structural Changes

Molecular dynamics simulations of the fully solvated variant I108T and WT cC were performed. We have carried out an analysis on the secondary and tertiary structural fluctuations/changes to explore how the single-site mutation influences the native state at the various structural levels. The total energy of the simulated systems was monitored to ensure energy conservation ($\Delta Etot/Etot < 0.002$).

Due to the Berendsen temperature coupling, total energy during 10ns in all simulations was completely conserved. The final temperature kept at 330 K as expected which indicated the simulated systems worked well.

In the experimental study of He *et al.*, fibrils were found favored to be produced in solutions of low pH, and the production was accelerated by high temperature (11). In addition, it has been proved that in MD simulations, high temperature and low pH value can accelerate protein unfolding without changing the pathway of unfolding (30). Therefore, we performed the simulations under the extreme conditions with the elevated temperature of 330 K and pH 2, to correspond with the conditions that were chosen in the experiment by He *et al.,* and further make the system reach the equilibrated regions at a minimum of simulation time and computational expense.

The overall stability of these monomers was evaluated using the Cα root-mean-square deviation (RMSD) relative to the corresponding initial structure (Figure 1). When the system reached an equilibrated region, the average RMSD were 0.32 nm and 0.25 nm respectively for I108T and WT cC in the last 3 ns of the simulation.

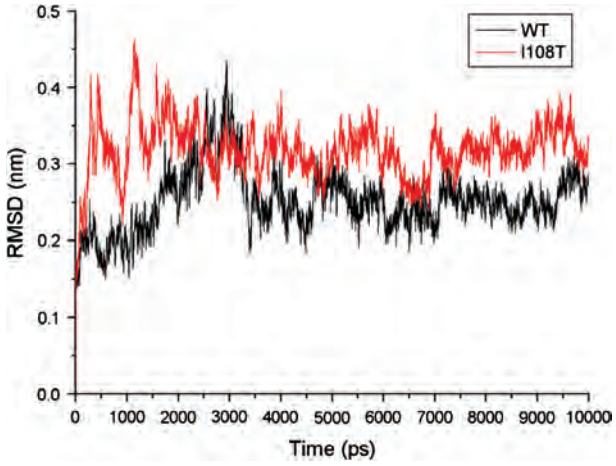

Figure 1: The Cα RMSD of the I108T mutant (*red*) and WT (*black*) cC as a function of simulation time.

"Final structure" mentioned in the following parts is defined as the average of the last 3ns, according to the equilibrium result. The RMSD value of both I108T and WT exceeded 0.2 nm, indicating the conformational changes have taken place during the simulations in both I108T and WT mutant cC. In addition, the RMSD value of I108T mutant was higher than WT cC monomer and exceeded 0.3, indicating that its secondary structure has probably changed. This suggested the increased structural change during the MD calculations of I108T mutant compared with WT cC was somehow related to amyloid fibril formation in cC. Although these structural changes of monomers are not dramatic at atomic level, there could be much more subtle influences in multi-molecules system.

Residue Averages of the RMSF in I108T

According to the RMSD value, the overall stability of the I108T mutant decreased compared with WT cC. We further analyzed the residue averages of the root mean square fluctuations (RMSF) during the MD simulations to find the key domain which induced the instability in I108T mutant.

In Figure 2 A, the RMSF for the Cα atoms was presented. Overall, for most residues of both I108T mutant and WT cC, the RMSF values were basically similar, and residues in AS region have obvious larger differences. The α2-helix which involved in AS region was nearly destroyed in I108T (decreased from 6 residues to 0, cal-

culated by DSSP algothrim), while it remained unchanged in WT cC (6 residues at the final state). Besides, another region that has slight difference is α1-helix, which is unchanged in I108T, while decreased from 15 residues to 13 residues in WT. This shortness in WT suggested that α1-helix might have the unfolding tendency in the extreme environment (330 K, pH 2). Threonine residue displaced isoleucine in I108T mutant cC prevented neighbored α1-helix in three dimensional from unfolding. This speculation can be further validated because the α1-helix in I66Q also decreased to 13 residues in another study conducted by us (unpublished data).

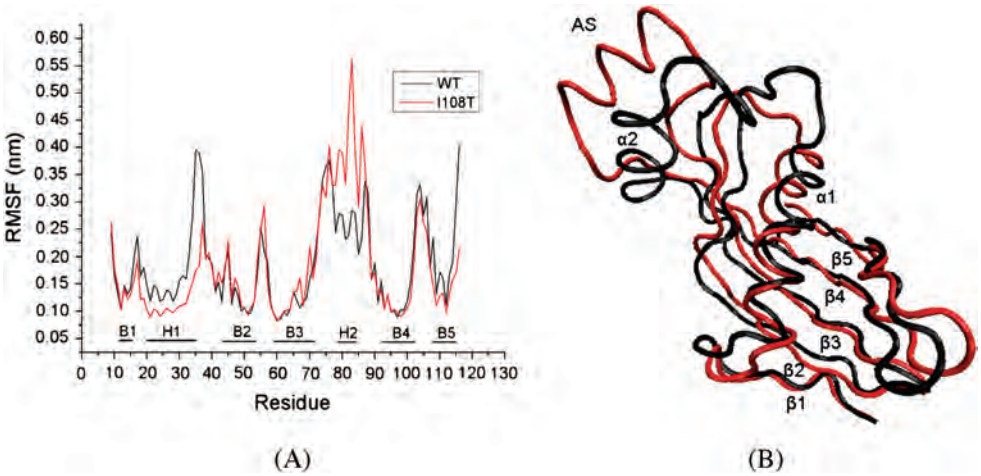

Figure 2: (**A**) The residue averages of the RMSF for the Cα atoms of I108T mutant (*red*) and WT (*black*) cC during the 10ns MD simulations. (**B**) Superposition of the Cα atoms of I108T mutant (*red*) and WT (*black*) cC structures at the end of the 10ns MD simulation.

For further observation of the structural changes in I108T mutant cC, we applied a visual analysis by superimposing alignment with VMD program. The final structure (after MD simulations) of I108T mutant was superimposed with the corresponding final structure of WT cC for the Cα. In I108T mutant cC, the AS region showed a large displacement (residue shift 0.27 nm referred to WT cC). The AS region including the untwisted α2-helix turned beyond the protein domain. α2-helix, which unfolded to turns, had a residue shift value of 0.26 nm, referred to WT cC, outside protein domain. The similar residue shift values between α2-helix and AS region illustrated that α2-helix had the same movement as the whole AS region. It suggested that the function deficiency of α2-helix probably related to the large displacement of AS region in I108T mutant cC.

According to the results of RMSF and superposition, the content and stability of α-helix decreased largely for the whole structure. It suggested the helix unfolding process has somehow related to amyloid fibril formation in cC.

Generally, a representative character of amyloid protein is the increasing of β-sheet while decreasing of α-helix content in the secondary structure (31, 32), which the character I66Q mutant just had (15). Interestingly, I108T mutant cC did not show obvious β-sheet decreasing detected by CD method in our previous experimental study (11). The data did not correspond with the secondary structure changes in amyloid protein in general.

Although CD spectroscopy can be used to study how the secondary structure of a molecule changes as a function of the various denaturing agents, it cannot get the dynamics character of the structural changing process. In order to get the detailed information of the secondary structure changes in I108T mutant and WT cC, we defined the content of α-helix and β-sheet as a function of simulation time by DSSP algothrim (Figure 3).

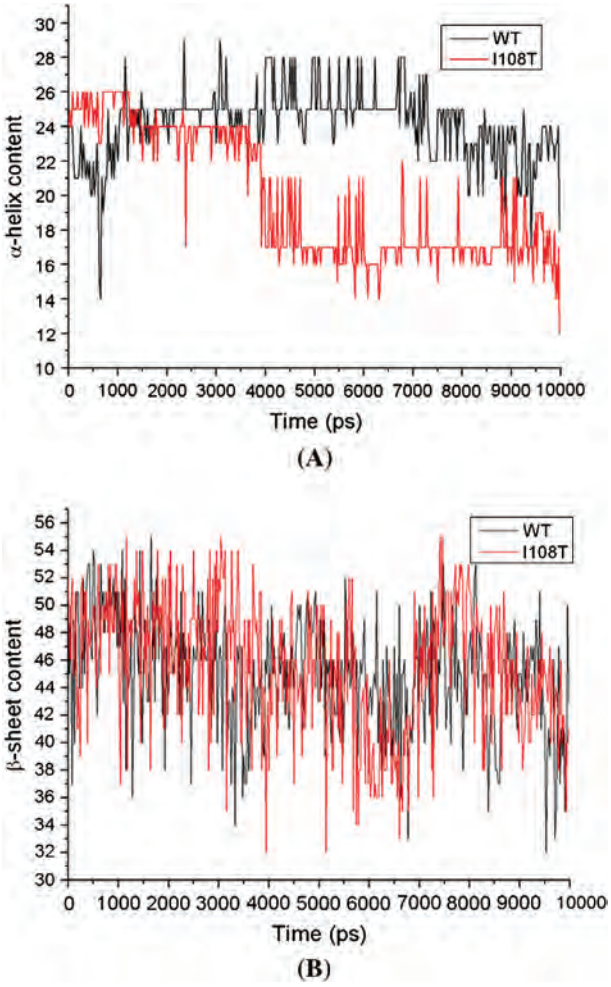

Figure 3: The content of α-helix (**A**) and β-sheet (**B**) in I108T mutant (*red*) and WT (*black*) cC as a function of simulation time.

Our MD simulation results are in accordance with the experimental data in our previous study (11, 15) (Figure 3). In our MD simulations, initially, the α-helix contents were 22% (24 residues) in both I108T and WT cC. Next, a notable decrease of α-helix content for I108T mutant can be seen around 4ns. The α-helix content in I108T mutant dramatically decreased to 16% (17 residues). While in WT cC, that was 21% (23 residues) slightly altered at the final structure. To observe the α-helix unfolding event at 4ns moment, we applied a movie of I108T mutant cC dynamics (movie not shown). At the point of 4.2ns, AS region including α2-helix had a sudden displacement outside the protein domain. Without the protection of neighboring domains, α2-helix is most likely unwound in the extreme solvent environment. The α2-helix unfolding event (6 residues to 0) is the reason why the α-helix content decreased around 4ns in Figure 3 A. Interestingly, in our MD simulations, the β-sheet content was slightly decreasing (Figure3 B). In I108T mutant cC, it changed from 48% to 43% (52 residues to 46 residues) at the end of the 10ns simulations. In WT cC, the β-sheet content changed from 48% to 44% (52 residues to 48 residues). By determining the secondary structure changes during the whole simulation time by DSSP, we found that the decreasing of β-sheet content was caused by the shortening of β2 and β3 in I108T mutant and WT cC. While in I108T mutant, β5 also tended to shorten because of the site mutation.

By observing the β-sheet content curve, we found that it shook dramatically between the value of 32 and 56 residues during the whole 10ns simulations, both in WT and I108T mutant cC. The large and frequent shaking suggested the β-sheet structure was extremely unstable. It should be protected by some structural factors, for instance neighboring domains or disulfide bonds and so on. The factors may keep the dynamic equimbrium of the β-sheet forming and unfolding process. In the extreme simulation environment we set, the factors are similar in WT and I108T mutant cC. That is the reason why the β-sheet content of I108T mutant is similar to WT cC. The shaking curves suggested the β-sheet tended to change, once the distinct factors changed in this extreme environment. The detailed information of the factors is not discussed in this article, and a further study on β-sheet restrict factors is in progress.

The secondary structure analysis referred to experiment data was illustrated in Table I. As described before, the secondary structure changes were corresponding well with the X-ray crystallography and CD spectroscopy data, both in α-helix and β-sheet. This also validated the accuracy of the MD simulation data from the perspective of molecular biology experiment. It can provide the basis for further study on more detailed information using MD simulation that cannot be obtained from the molecular biology experiment.

Table I

The content of α-helix and β-sheet in our MD simulations compared with the experimental data in previous studies.

	MDs*[1]		experimental*[2]	
	α-helix content	β-sheet content	α-helix content	β-sheet content
WT	21%	44%	22%*3	48%*3
I108T	16%	43%	17%*4	48%*4

*[1]330 K, pH=2 *[2]298 K, pH=7 *[3] the data determined by X-ray(2) *[4] the data determined by CD spectroscopy which referenced to the X-ray data of WT(11)

The interior hydrophobic core of cystatin provides the structural stability favoring the native state during the protein folding (2, 33). According to the hypothesis in previous study, hydrophilic residues in hydrophobic core mutated to hydrophobic, making the hydrophilic residues expanded, exposing inner hydrophobic core to hydrophilic solvent environment which enhanced the intermolecular hydrophobic interaction. This may cause the destabilization of the molecular α/β interface, leading to structural rearrangements and intermolecular domain swapping, and then induce the amyloid aggregation (5, 14, 34). The L68Q mutant in HCC and I66Q mutant cC might form highly domain-swapped dimers by such a mechanism (4, 5, 11, 13).

In the case of cC, Val 14, segment Leu21-Met29 of H1, and segments Val44-Ala50, Leu62-Ile66, Thr93-Val99 and Ile108-Cys115 of β-strands 2-5 participate through their side chains in the formation of a hydrophobic molecular core (2). What has attracted our attention is that, similar to residue 66, residue 108 (located in β5) was also located in the hydrophobic core in cC. It strongly suggested that the mechanism in which the site mutation of 108 has caused the amyloid aggregation might be similar to the site mutation of 66.

To analyze the behavior of the hydrophobic core in I108T mutant cC, we determined the structure drift and the side chain surface of the hydrophobic core throughout the MD simulations. Through the comparison of the hydrophobic core structure drift of WT and I108T mutant (Figure 4 A and B), we can learn that, in extreme conditions, the hydrophobic core of I108T was more flexible and free than WT cC, indicating that the hydrophobic core of I108T mutant was more unstable.

In WT cC, the hydrophilic residues (109, 23, 46) of the hydrophobic core have slightly expanded, and the inner hydrophobic residues (110, 115) surrounded by the outer hydrophilic residues have expanded slightly beyond. We believed that such slight change is caused by the extreme conditions. While in I108T mutant cC, compared to WT, the outer hydrophilic residues (109, 23, 26 and 46) expanded dramatically, to the solvent environment by the enhancement of hydrophilic Thr

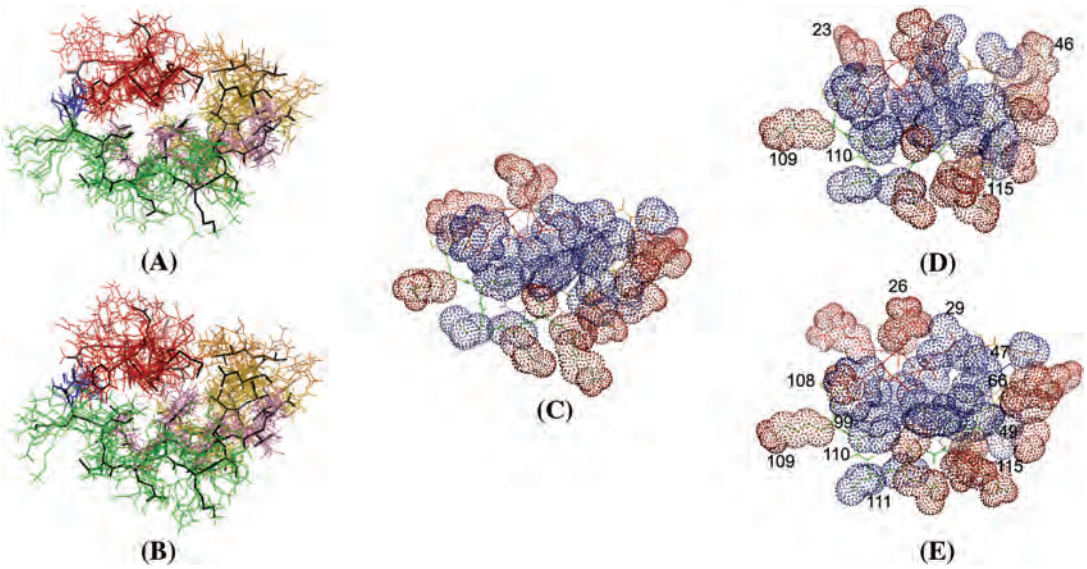

Figure 4: The hydrophobic core structures of cC. (**A**), (**B**) Superimpositions of the hydrophobic core snapshots of wt and I108T mutant cC, respectively. (black for the reference structure, red for β1, orange for β2, gold for β3, pink for β4, green for β5 and blue for the 108 residue. (**C**) The initial structure of the hydrophobic core of cC. (**D**), (**E**) Structure of the hydrophobic core of WT and I108T mutant cC respectively after 10ns simulation; In (**C**), (**D**) and (**E**), red indicate the hydrophilic residues and the blue indicate the hydrophobic residues.

resiude at 108 site. Inner hydrophobic core extended outside to the solvent obviously (29, 45, 47, 49, 66, 99, 110, 111 and 115). The result is just in accordance with the hypothesis in previous study.

According to both the experimental results on CD spectroscopy, thioflavin T fluorescence value, EM data and the MD simulation results, I108T mutant exhibited a series of obvious amyloid characters. However, compared to the highly amyloidogenic I66Q mutant, the I108T is an atypical amyloidgenic protein: i) the amyloid fibrils formation in I108T is not as significant as in I66Q; ii) the secondary structural changes are not as obvious as in I66Q and iii) the hydrophobic core expanding tendency in I108T are not as dramatic as in I66Q. Moreover, our simulation data in I108T study provided the potent evidence to the hypothesis that the mutations in the hydrophobic core might be closely associated with the amyliodsis formation. Meanwhile, the results strongly suggested that mutants with site mutation of other hydrophobic residues in the hydrophobic core might also be the amyloidgenic-prone mutation through the similar mechanism. Further study in the mutation of these sites will be helpful to illustrate the domain swapping mechanism of the amyloid aggregation.

Acknowledgment

This work was supported by the key laboratory foundation (No. 20085100) and foundation (No. 20060358) from Liaoning Provincial Education Department. Partially supported by National Science Foundation of China (No. 30600113), Natural Science Foundation of Liaoning Province (No. 20072055) and foundation (No. 1063305-1-00) from Bureau of Science and Technology of Shenyang. We thank Prof. Dongqing Wei of Shanghai Jiaotong University for his kind support and helpful discussion.

References and Footnotes

1. M. Abrahamson, A. Ritonja, M. A. Brown, A. Grubb, W. Machleidt, and A. J. Barrett. *J Biol Chem 262,* 9688-9694 (1987).
2. W. Bode, R. Engh, D. Musil, U. Thiele, R. Huber, A.Karshikovl, J. Brzin, J. Kos, and V. Turk, *EMBO J 7*, 2593-2599 (1988).
3. O. Jensson, G. Gudmundsson, A. Arnason, H. Blöndal, I. Petursdottir, and L. Thorsteinsson, *et al., Acta Neurol Scand 76*, 102-114 (1987).
4. I. Olafsson and A. Grubb. *Amyloid 7*, 70-79 (2000).
5. R. Janowski, M. Kozak, E. Jankowska, Z. Grzonka, A. Grubb, M. Abrahamson, and M. Jaskolski. *Nat Struct Biol 8*, 316-320 (2001).
6. M. Abrahamson, and A. Grubb, *Proc Nati Acad Sci 91*, 1416-1420 (1994).
7. M. Bjarnadottir, C. Nilsson, V. Lindstrom, A. Westman, P. Davidsson, F. Thormodsson, H. Blondal, G. Gudmundsson, and A. Grubb. *Amyloid 8*, 1-10 (2001).
8. A. Sanders, C. Jeremy Craven, L. D. Higgins, S. Giannini, M. J. Conroy, A. M. Hounslow, J. P. Waltho, and R. A. Staniforth. *J Mol Biol 336*, 165-178 (2004).
9. R. A. Staniforth, S. Giannini, L. D. Higgins, M. J. Conroy, A. M. Hounslow, R. Jerala, C. J. Craven, and J. P. Waltho. *EMBO J 20*, 4774-4781 (2001).
10. A. Sanders, C. C. Jeremy, L. D. Higgins, S. Giannini, M. J. Conroy, A. M. Hounslow, J. P. Waltho, and R. A. Staniforth. *J Mol Biol 336*, 165-178 (2004).
11. J. W. He, Y. T. Song, N. Ueyama, A. Saito, H. Azakami, and A. Kato. *Protein Sci 15*, 213-222 (2006).
12. R. Engh, T. Dieckmann, W. Bode, E. A. Auerswald, V. Turk, R. Huber, and H. Oschkinat. *J Mol Biol 234*, 1060-1069 (1993).
13. S. Rodziewicz-Motowidio, M. Wahlbom, X. Wang, J. Gagiewka, R. Janowski, M. Jaskólski, A. Grubb, and Z. Grzonka. *J Struct Biol 154*, 68-78 (2006).
14. H. L. Liu, Y. M. Lin, J. H. Zhao, M. C. Hsieh, H. Y. Lin, C. H. Huang, H. W. Fang, Y. Ho, and W. Y. Chen. *J Biomol Struct Dyn 25*, 135-144 (2007).
15. J. W. He, Y. T. Song, N. Ueyama, A. Harada, H. Azakami, and A. Kato. *J Biochem 137*, 477-485 (2005).
16. H. L. Zhang, Y. Liu, Y. Y. Yu, B. J. Hu, and Y. T. Song. *J of Liaoning Technical University (Natural Science) 27*, 472-474 (2008).
17. K. Arnold, L. Bordoli, J. Kopp, and T. Schwede. *Bioinformatics 22*, 195-201 (2006).
18. T. Schwede, J. Kopp, N. Guex, and M. C. Peitsch. *Nucleic Acids Research 31*, 3381-3385 (2003).

19. N. Guex and M. C. Peitsch. *Electrophoresis 18*, 2714-2723 (1997).
20. H. J. C. Berendsen, D. van der Spoel, and R. van Drunen. *Comput Phys Commun 91*, 43-56 (1995).
21. E. Lindahl, B. A. Hess, and D. van der Spoel. *J Mol Model 7*, 306-317 (2001).
22. D. van der Spoel, E. Lindahl, B. Hess, G. Groenhof, A. E. Mark, and H. J. C. Berendsen. *J Comput Chem 26*, 1701-1718 (2005).
23. B. Hess, C. Kutzner, D. van der Spoel, and E. Lindahl. *J Chem Theory Comput 4*, 435-447 (2008).
24. W. F. van Gunsteren, S. R. Billeter, A. A. Eising, P. H. Hünenberger, P. Krüger, A. E. Mark, W. R. P. Scott, and I. G. Tironi. *Hochschuleverlag AG an der ETH Zürich, Zürich,* (1996).
25. T. Darden, D. York, and L. Pedersen. *J Chem Phys 98*, 10089-10092 (1993).
26. U. Essmann, L. Perera, M. L. Berkowitz, T. Darden, H. Lee, and L. G. Pedersen. *J Chem Phys 103*, 8577-8592 (1995).
27. H. J. C. Berendsen, J. P. M. Postma, W. F. van Gunsteren, and J. Hermans. *D Reidel Publishing Co, Dordrecht,* 331-342 (1981).
28. W. Kabsch and C. Sander. *Biopolymers 22*, 2577-2637 (1983).
29. W. Humphrey, A. Dalke, and K. Schulten. *J Molec Graphics 14*, 33-38 (1996).
30. R. Daya, B. J. Benniona, S. Hama, and V. Daggett. *J Mol Bio 322,* 189-203 (2002).
31. J. Kelly. *Curr Opin Struck Biol 8*, 101-106 (1998).
32. M. Stefani, C. M. Dobson. *J Mol Med 81*, 678-699 (2003).
33. J. H. Zhao, H. L. Liu, Y. F. Liu, H. Y. Lin, H. W. Fang, Yi. Ho, and W. B. Tsai. *J Biomol Struct Dyn 26*, 481-490 (2009).
34. M. Nilsson, X. Wang, S. Rodziewicz-Motowidlo, R. Janowski, V. Lindström, P. Ö nnerfjord, G. Westermark, Z. Grzonka, M. Jaskolski, and A. Grubb. *J Biological Chem 279*, 24236-24245 (2004).
35. L-K. Chang, J-H. Zhao, H-L. Liu, K-T. Liu, J-T. Chen, W-B. Tsai, and Y. Ho. *J Biomol Struct Dyn 26,* 731-740 (2009).
36. Po-S. Fang, J-H. Zhao, H-L. Liu, K-T. Liu, J-T. Chen, H-Y. Lin, C-H. Huang, and H-W. Fang. *J Biomol Struct Dyn 26,* 549-560 (2009).
37. F. Mehrnejad and N. Chaparzadeh. *J Biomol Struct Dyn 26,* 255-262 (2009).
38. J. Yoon, J. Park, S. Jang, K. Lee, and S. Shin. *J Biomol Struct Dyn 27,* 259-270 (2009).
39. J. Yoon, J. Park, S. Jang, K. Lee, and S. Shin. *J Biomol Struct Dyn 25,* 505-516 (2008).

Date Received: August 6, 2009

Communicated by the Editor Ramaswamy H. Sarma